High birefringence in elliptical hollow optical fiber

In-Kag Hwang and Yong-Hee Lee

Department of Physics, Korea Advanced Institute of Science and Technology
Daejeon, 305-701, Korea
ikhwang@kaist.ac.kr

Kyunghwan Oh

Department of Information and Communications, Gwangju Institute of Science and Technology
Gwangju, 500-712, Korea

David N. Payne

Optoelectronic Research Centre, University of Southampton
Southampton SO17 1BJ, United Kingdom

Abstract: We propose a novel design of highly birefringent optical fiber composed of a central elliptical air hole, a circumferential elliptical ring core, and a circular cladding. The proposed waveguide structure is predicted to produce a linear birefringence higher by an order of magnitude than the solid elliptical core fiber. The large index contrast between the central air and germanosilica elliptical ring core is mainly attributed to the high birefringence and its characteristics are theoretically analyzed in terms of its waveguide parameters.

OCIS codes: (060.2420) Fibers, polarization-maintaining; (260.1440) Birefringence

References and links

1. R. A. Bergh, H. C. Lefervre, and H. J. Shaw, "An overview of fiber-optic gyroscopes," J. Lightwave Technol. **2,** 91-107 (1984).
2. M. Nakazawa, "Highly efficient Raman amplification in a polarization-preserving optical fiber," Appl. Phys. Lett. **46,** 628-630 (1985).
3. R. B. Dyott, J. R. Cozens, and D. G. Morris, "Preservation of polarization in optical-fiber waveguides with elliptical cores," Electron. Lett. **15,** 380-382 (1979).
4. T. Hosaka, K. Okamoto, T. Miya, Y. Sasaki, and T. Edahiro, "Low-loss single polarization fibers with asymmetrical strain birefringence," Electron. Lett. **17,** 530-531 (1981).
5. L. Poti, and A. Bogoni, "Experimental demonstration of a PMD compensator with a step control algorithm," IEEE Photon. Technol. Lett. **13,** 1367-1369 (2001).
6. C. C. Renaud, H. L. Offerhaus, J. A. Alvarez-Chavez, J. Nilsson, W.A. Clarkson, P. W. Turner, D. J. Richardson, and A. B. Grudinin, "Characteristics of Q-switched cladding-pumped Ytterbium-doped fiber lasers with different high-energy fiber designs," IEEE J. Quantum Electon. Lett. **37,** 199-206 (2001).
7. S. Choi, K. Oh, W. Shin, C. S. Park, U. C. Paek, K. J. Park, Y. C. Chung, G. Y. Kim, and Y. G.. Lee, "Novel Mode Converter Based on Hollow Optical Fiber for Gigabit LAN Communication," IEEE Photon. Technol. Lett. **14,** 249-250 (2002).
8. S. Choi, W. Shin, and K. Oh, "Higher-order-mode dispersion compensation technique based on mode converter using hollow optical fiber," in *Proc. Optical Fiber Communication Conference 2002* (Optical Society of America, Washington, D.C., 2002), pp. 177-178.
9. S. Choi, T. J. Eom, J. W. Yu, B. H. Lee, and K. Oh, "Novel all-fiber bandpass filter based on hollow optical fiber," IEEE Photon. Technol. Lett. **14,** 1701-1703 (2002).
10. S. G. Johnson and J. D. Joannopoulos, "Block-iterative frequency-domain methods for Maxwell's equations in a planewave basis," Opt. Express **8,** 173-190 (2001), http://www.opticsexpress.org/abstract.cfm?URI=OPEX-8-3-173.
11. Y.-J. Lee, D.-S. Song, S.-H. Kim, J. Huh, and Y.-H. Lee, "Modal Characteristics of photonic crystal fibers," J. Opt. Soc. Korea **7,** 47-52 (2003).

#3984 - $15.00 US Received 5 March 2004; revised 19 April 2004; accepted 20 April 2004

12. I.-K. Hwang, Y.-J. Lee, and Y.-H. Lee, "Birefringence induced by irregular structure in photonic crystal fiber," Opt. Express **11,** 2799-2806 (2003), http://www.opticsexpress.org/abstract.cfm?URI=OPEX-11-22-2799.

1. Introduction

High birefringence fibers (Hi-Bi fiber) or polarization maintaining fibers (PMF) have been widely used for polarization control in fiber-optic sensors, precision optical instruments, and optical communication systems [1,2]. In these fibers, the two eigen polarization modes propagate with their own propagation constants due to a relatively large effective index difference between the modes, or equivalently high birefringence. High birefringence in optical fibers has been usually achieved either by asymmetric shape in waveguide, such as an elliptical core[3], or by asymmetric stress distribution around the core incorporating the stress-applying-parts (SAP)[4].

In recent high data rate optical communications, especially for 40 Gbps systems, first order polarization mode dispersion (PMD) compensation techniques requires PMFs to utilize its differential group delay between the two eigen polarization states [5]. In order to enhance the figure of merit in PMD compensation, large differential group delay, or equivalently high birefringence, is required along with a low propagation loss. A new technique to induce high birefringence in optical fiber, therefore, would give a significant impact on optical communication based on 40 Gbps systems and beyond.

Polarization maintenance is also one of critical issues in recent clad pumped fiber laser (CPFL) cavities, where a good overlap between signal photon in the core and pump in the cladding is crucial along with output requirements such as single mode and sing polarization [6]. Conventional PANDA or Bow-tie type birefringent fibers, however, have SAPs whose refractive indices are significantly different from both the core and the silica cladding. If used in CPFL cavities, those conventional PMFs based on SAP will severely deteriorate the overlap between the signal in the core and pump in the cladding, which subsequently decreases the output power and pump efficiency.

In conventional elliptical core fibers, the birefringence primarily comes from the core ellipticity and the index difference between the core and the cladding. The cladding does not include SAP such that the clad pumping scheme in fiber lasers can be adopted. However, a large index difference over 0.02 is generally required to achieve a birefringence > 10^{-4} [3] and high GeO_2 concentration subsequently induces high propagation loss over several dB/km. Furthermore, the high index difference between the core and cladding imposes significant limitations on the overlap between the signal and pump.

It is, therefore, highly desirable to generate a large birefringence with a low scattering loss, usually associated with the core refractive index, yet without significant perturbations in the cladding modes to cope with recent challenges and demands in fiber optic polarization control.

Recently a new type of optical fiber, hollow optical fiber (HOF), with a triple layered structure, a central air hole, germanosilica ring core, and silica cladding has been proposed for versatile photonic device applications [7-9]. HOF inherently possesses high compatibility with conventional SMFs due to its capability to form a low loss adiabatic mode conversion. The high index contrast between the central air hole and the glass ring core can be utilized for polarization control, while the light is mainly guided by the index difference between the ring core and the cladding.

In this paper, we propose a novel design of highly birefringent fiber by introducing an elliptical air hole and concentric circumferential elliptical ring core. Due to the large contrast in the refractive index between the ring core and the air hole, high birefringence can be achieved with a relatively small index difference between the core and the cladding. Since SAP was not introduced, the proposed fiber does not disturb the cladding modes in CPFLs. The fiber could, therefore, serve as an ideal PMF with a high birefringence and low loss for PMD compensation as well as polarization maintaining CPFL cavity. The central air hole and

#3984 - $15.00 US Received 5 March 2004; revised 19 April 2004; accepted 20 April 2004

its asymmetry could endow a new degree of freedom to design the birefringence in optical waveguides. In this paper the origin of the birefringence is discussed and its dependence on the structural parameters is analyzed in the proposed elliptical hollow optical fiber (E-HOF), for the first time to the best knowledge of the authors.

2. Origin of high birefringence

The proposed structures of the E-HOF are shown in Fig. 1, along with major waveguide parameters. An elliptical air hole at the center is concentric to the circumferential elliptical ring core. Note that the index difference between the central air hole and the ring core is over 0.45, while the difference between the core and cladding is represented by Δn.

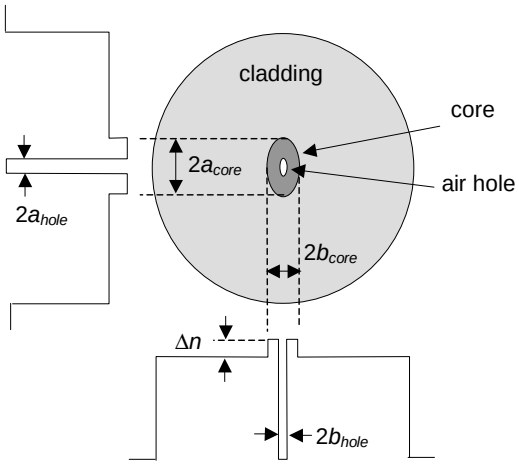

Fig. 1. The cross section of the proposed elliptical hollow optical fiber. The elliptical air hole is concentric to the elliptical ring core. Key waveguide parameters are; the major axes of the air hole, and the ring core, a_{hole}, and a_{core}, the minor axes, b_{hole}, and b_{core}, the refractive index difference of core and cladding, Δn.

The birefringence in the proposed fiber originates from the boundary conditions for electromagnetic fields at the elliptical core-hole interface. At the interface of two different linear, homogeneous, and isotropic dielectrics, the Maxwell's equations impose the boundary conditions for the normal and the transverse components of electric fields.

$$E_{1t} = E_{2t} \tag{1}$$

$$D_{1n} = D_{2n} \quad or \quad n_1^2 E_{1n} = n_2^2 E_{2n} \tag{2}$$

where the subscript numbers denote each dielectric, and the subscript t and n denote the transverse and the normal components of the fields, respectively.

When these boundary conditions are applied to the elliptical air-core interface, the electric fields show significantly different distributions for the two orthogonal polarization directions. Fig. 2 shows the electric field distribution for two polarizations, parallel to *x* and *y* axes in the proposed E-HOF. A significant difference in intensity distribution between (a) an (b) is observed at the air hole region, which is magnified in (a') and (b'), respectively. For the *y*-polarized mode in Fig. 2(a'), the electric fields are tangential to the boundary at the left and the right sides of the hole along the major axis of the ellipse, and the amplitude of the electric field should be continuous across this boundary from Eq. (1). However, at the top and the bottom the air-core interface along the minor axis, the electric fields are normal to the boundary and Eq. (2) forces the discontinuity of the electric fields across the boundary. At this boundary, the electric field amplitude in the core is reduced by the large refractive index ratio, $(n_{air}/n_{core})^2 \approx 0.46$, resulting in depression of electric field intensity near the top and bottom sides of the hole. On the other hand, for the *x*-polarized mode in Fig. 2(b'), the discontinuity

#3984 - $15.00 US Received 5 March 2004; revised 19 April 2004; accepted 20 April 2004

occurs at the left and right sides of the hole along the major axis. The intensity disparity around the interface is more substantial in the *x*-polarized mode due to the longer effective boundary length along the major axis. In *x*-polarization we could, therefore, observe more prominent depression in the electric field intensity, see Fig. 2(b) near the air-core interface. The preceding arguments could be also applied to the elliptical core-silica cladding boundary, but the subsequent disparity in electric field distribution is very minor to be visualized in (a) and (b) due to relatively small index difference between the core-cladding.

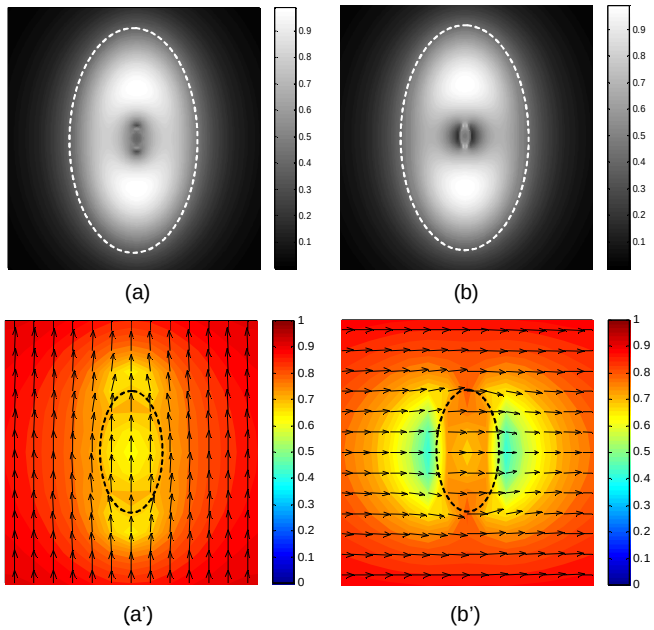

Fig. 2. The electrical field profiles of (a) *y*- and (b) *x*-polarization modes. The white dashed curve indicates the core-cladding boundary. The core-cladding index difference was set to be 0.02. The central air hole regions are magnified in (a') and (b') to show the details. The black dashed curve indicates the elliptical air-core interface. The color level and the arrows denote the amplitude and the direction of the electric field, respectively. Note that electric field amplitude in the x-polarization is more significantly suppressed at the interface than that in the y-polarization.

The electric field intensity distribution is directly related to the effective index of the guided mode such that the *x*-polarization mode with more prominent intensity suppression around the hole as shown in Fig. 2(b) will result in a lower effective index than the *y* polarization making *x* and *y* axes as the fast and the slow axes, respectively. Birefringence in this proposed E-HOF can be further enhanced by maximizing the polarization dependent disparity in the electric field intensity distribution around the air-core interface, which is achieved by optimizing waveguide parameters such as the core-cladding index difference, ellipticity, and hole size.

The proposed fiber structure can provide an optimal birefringent optical medium in the notions that 1) it can utilize the high refractive index difference between the air and germanosilicate ring core, and 2) it can alleviate the requirement for high Δn between the core and cladding to provide a low scattering loss and flexible design for active fiber devices. Note that the available index difference between the core and cladding in the conventional solid elliptical core fiber is limited below 0.04 due to germanium incorporation chemistry in silica glass. On the while in the proposed E- HOF the index difference of the air-core boundary is as high as ~ 0.45, an order of magnitude larger than solid elliptic core fibers, which can

#3984 - $15.00 US Received 5 March 2004; revised 19 April 2004; accepted 20 April 2004

potentially produce extraordinarily high birefringence. Furthermore, the core radius should significantly decrease according to the high Δn requirement in the conventional elliptical core fiber to maintain the normalized frequency, V, below the higher-order mode cutoff. However, in this new approach, the birefringence is mainly produced by the central air hole and the dimension of the ring core can be further controlled to provide a larger effective mode area without significantly affecting the V value.

3. Numerical analyses of the birefringence of E-HOF

The dispersion curves and the birefringence of the two polarization modes were computed using a plane-wave expansion method. Fully-vectorial eigenmodes of Maxwell's equations with periodic boundary conditions were computed by preconditioned conjugate-gradient minimization of the block Rayleigh quotient in a plane-wave basis, using a freely available software package [10,11]. The number of plane waves used for the computation was 840×840. The error due to the finite number of the plane waves in calculation of the birefringence was confirmed to be less than 10% [12]. In the simulation, the cladding diameter was set to be ~ 6 times of the major-axis of the core in order to facilitate rapid calculation and it was confirmed that the cladding dimension is still large enough not to affect the dispersion of the core modes in the range of interests.

The refractive indices of the air, cladding, core were set as n_{air}=1, n_{clad}=1.45, n_{core}=1.45+Δn, respectively. The semi-major axis (a) and ellipticity (1-b/a) of the hole and the core, as well as the core-cladding index difference (Δn), are the key parameters determining the birefringence. In this analysis we first considered the case for the ellipticity of 0.5 such that b/a=0.5 for both the air hole and the ring core.

The birefringence is plotted as a function of the normalized frequency, V, in Fig. 3(a) and (b) for Δn=0.01 and Δn=0.02, respectively. Here the normalized frequency V_{ab} is defined as

$$V_{ab} = \frac{2\pi\sqrt{a_{core}b_{core}}}{\lambda}\sqrt{n_{core}^{\ 2} - n_{clad}^{\ 2}} \approx \frac{2\pi a_{core}}{\lambda}\sqrt{n_{clad}\cdot\Delta n} \qquad (3)$$

where a_{core} and b_{core} are the semi-major and semi-minor axes of the elliptic core, and b_{core}/a_{core}=0.5. The hole size is represented as a ratio to the core size, a_{hole}/a_{core}. The curves for a_{hole}/a_{core} =0 correspond to the conventional solid elliptical core fiber, which agrees well with prior simulations found in Ref. [3].

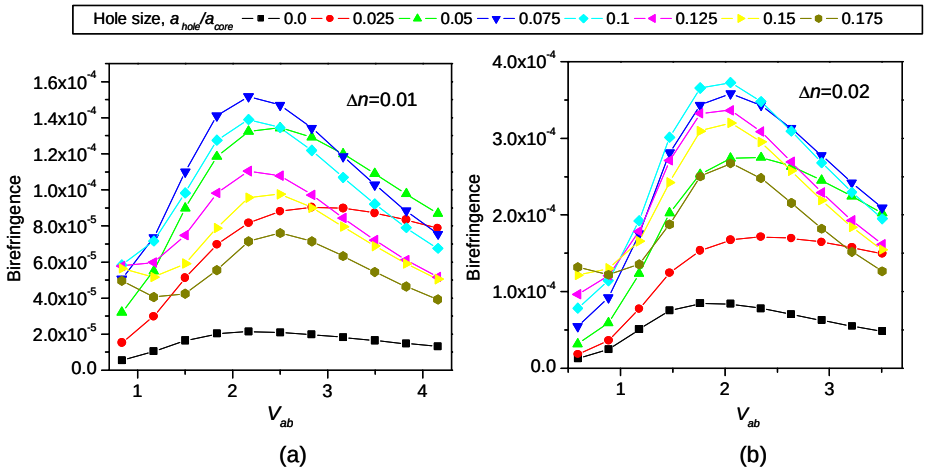

Fig. 3. Birefringence as a function of normalized frequency, V_{ab}. Each curve corresponds to each hole size, a_{hole}/a_{core}. The core-cladding index differences, Δn, are (a) 0.01 and (b) 0.02.

In Fig. 3, two notable birefringent features have been observed. Firstly, the maximum birefringence in each plot was found to be located near V_{ab} ~ 2 independent of the parameter,

#3984 - $15.00 US Received 5 March 2004; revised 19 April 2004; accepted 20 April 2004

a_{hole}/a_{core}, yet the birefringence of each fiber design did strongly depend on the hole size. Secondly, the maximum birefringence in the proposed fiber has increased by several folds compared to the conventional solid elliptical core fiber with the same waveguide parameters such as index difference, Δn, and ellipticity. For Δn of 0.01, the optimal hole size, a_{hole}/a_{core}, was 0.075, while in the case of Δn=0.02, the birefringence reached its maximum at a_{hole}/a_{core}=0.1. It is noteworthy to confirm that only a fraction of air hole in the core, could induce a drastic changes in polarization characteristics by the virtue of huge index difference between the air and the glass ring core.

As in the case of conventional elliptical core fibers, the first excited LP11 mode in the weakly guiding approximation is no longer degenerate to split into LP11x/y-even/odd modes in the proposed fiber. The cutoff for the first higher mode, LP11x-even, was found to be located near V_{ab}=2.5 and V_{ab}=2.1 for the case of Δn=0.01 and 0.02, respectively.

The optimal dimensions of the core and the air hole can be estimated from the observation of the numerical results in Fig. 3. The optimal semi-major axis of the core, a_{core}, is given by the condition V_{ab}=2 of Eq. (3) as

$$a_{core} = \frac{\lambda}{\pi\sqrt{n_{cl} \cdot \Delta n}}. \tag{4}$$

For λ=1550 nm, a_{core} is found to be 4.1 and 2.9 μm for Δn=0.01 and 0.02, respectively. The semi-minor axis can be computed from the ellipticity of 0.5. The optimal hole sizes are 0.31, and 0.29 μm for Δn=0.01 and 0.02, respectively.

Fig. 3 suggests that this new approach alleviates the requirement of Δn for high birefringence, which has been rather stringent in conventional elliptical solid core fibers. It also results in a larger core size for the same birefringence than the prior fibers, which can be inferred from Eq. (4). For example, birefringence of 2×10^{-4} at 1550 nm can be achieved with Δn=0.012 and a_{core}=3.74 μm by introduction of the air hole of a_{hole}=0.3 μm in the E-HOF. The same amount of birefringence in the conventional elliptical solid core fiber, on the while, would require Δn=0.031 and a_{core}=2.33 μm without the air hole. E-HOF, therefore, can achieve both the reduction of Δn and the increase of core area by several folds.

In order to find the dependence of the birefringence on the index difference, Δn, and the hole size, a_{hole}, birefringence curves for Δn=0.005 and 0.03 were further calculated. The maximum birefringence in each case is, then, plotted as a function of a_{hole} in Fig. 4. In this case, the relative hole size, a_{hole}/a_{core}, was replaced with a_{hole}/λ using Eq. (4).

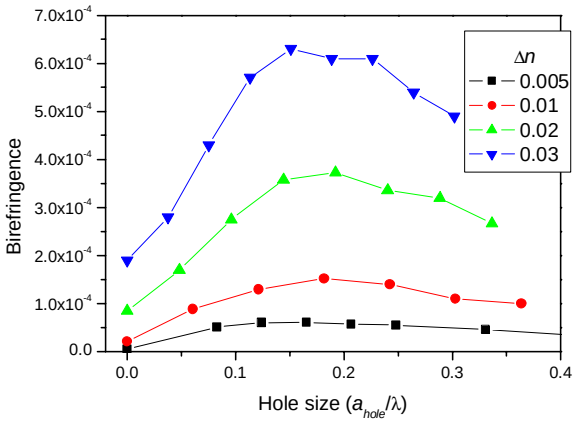

Fig. 4. The birefringence as a function of the hole size, a_{hole}/λ. Each curve corresponds to each Δn.

#3984 - $15.00 US
Received 5 March 2004; revised 19 April 2004; accepted 20 April 2004

It should be noted that the birefringence does not grow monotonically with the hole size and there exists an optimal a_{hole}, which is found to be a function of wavelength only.

$$a_{hole} \approx 0.18\lambda \tag{5}$$

The hole size dependence can be understood by investigating the electrical field distribution near the air-core interface. As discussed earlier, the magnitude of the birefringence is closely related to the disparity in the electric field intensity formed near air-core interface.(See Fig. 2.) When the hole is too small, its impact on the electric field intensity distribution is negligible to produce a low birefringence. As the hole size increases, the disparity appears over larger area producing higher birefringence. However, at an excessively large hole size, the optical power is strongly confined in the core region, only, leaving extremely weak optical intensity around the hole in both of the two polarization modes. The disparity between the two modes accordingly becomes insignificant, resulting in low birefringence. This explains the birefringence behavior depending on the hole size.

In the proposed E-HOF, the shape birefringence comes from two contributions, asymmetry at the core-cladding and the air-core boundaries. The former contribution can be inferred from the birefringence plots for the case of a_{hole}=0 in Fig. 4. The contribution from the air-core boundary can be obtained by subtracting the core-cladding contribution at a_{hole}=0 from the total birefringence assuming the magnitude of the first factor does not change with a_{hole}. The two contributions, together with the total birefringence, are plotted as functions of Δn in Fig. 5. The core-cladding boundary contribution grows proportional to Δn^2, which is a basic feature of elliptical core fibers [3]. On the other hand, the air-core boundary contribution was found to be linearly proportional to Δn. In the practical range of Δn, the contribution from the air-core boundary dominates that from the core-cladding boundary as expected. The linear dependence of the air-core boundary effect over Δn is also related to the optical intensity around the hole. Larger Δn and smaller core area provide the higher concentration of optical power at the center of the core, increasing the effect of the air hole boundary.

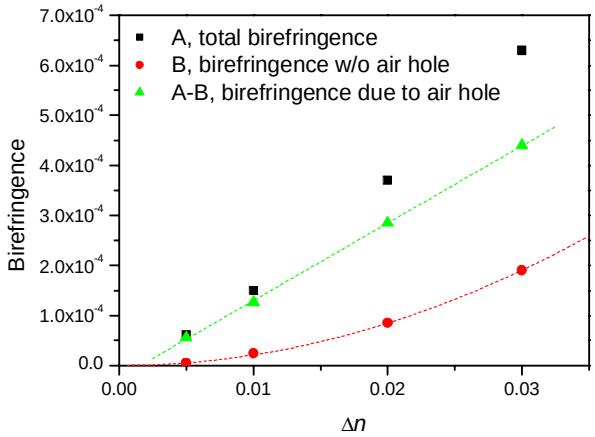

Fig. 5. The birefringence maxima achievable with each Δn: *A*, the maxima of the total birefringence from Fig. 5; *B*, the birefringence at a_{hole}=0; *A-B*, the birefringence due to the core-air boundary effect. The data in diamonds and triangles symbols are fitted with a parabolic and a linear function, respectively.

The contribution of the air-core boundary could be selectively calculated, in a different way from above, by computing the birefringence in the circular-core elliptical-hole fiber structure. The same linear relation between the index difference and the birefringence was obtained with a slope close to the line (A-B) in Fig. 5, which verifies the mutual independency of the two contributions.

#3984 - $15.00 US
Received 5 March 2004; revised 19 April 2004; accepted 20 April 2004

The birefringence as a function of the ellipticity was also investigated and shown in Fig. 6. The ellipticity of the core and the hole varied simultaneously, and the optimal hole sizes were estimated from Eq. (5) to obtain the maximum birefringence. The birefringence increases almost linearly with the ellipticity, at the different slopes depending on the index difference, Δn, as expected.

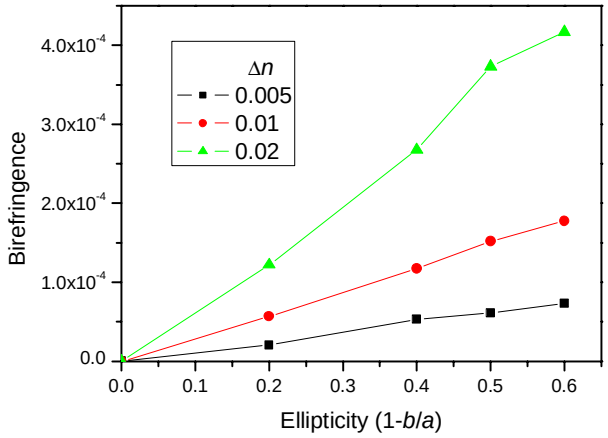

Fig. 6. The birefringence as a function of ellipticity. The ellipticity of the hole and the core was varied simultaneously. Each curve corresponds to each Δn.

The mode profile of E-HOF shown in Fig. 2 has an intensity dip at the center of the core. When this fiber is directly coupled to a conventional single mode fiber with a circular core, there could be considerable loss due to the mismatch of the mode profiles between the two fibers. However, it has been observed that when a HOF is locally heated, the air hole collapses to a solid core producing an adiabatic mode transformer [7], which can significantly reduce the splice loss to SMFs.

In general, the small Δn spreads the guided optical field further out to the cladding and results in a larger mode overlap between the core and the cladding modes. The proposed E-HOF can take advantage of the overlap control and will be very useful when a large mode overlap is necessary such as in long-period gratings or in cladding-pumped fiber lasers.

4. Conclusion

A novel design for high birefringence fiber incorporating an elliptical hole in the core was proposed and numerically analyzed. The large index contrast between the core and the air resulted in the birefringence about an order of magnitude higher than that from the solid elliptic core fiber based on the core-cladding index contrast. The maximum birefringence was achieved near $V_{ab} \sim 2$ independent of waveguide parameters. The optimal hole size for the maximal birefringence was found to be proportional to the wavelength, $a_{hole} \approx 0.18\lambda$. The birefringence due to the air-core boundary contribution was found to be linearly proportional to the core-cladding index difference, Δn. The proposed E-HOF could significantly reduce the requirements for high Δn, and small core area in the conventional elliptical solid core fibers, which endows a new degree of freedom to control the core-cladding mode overlap function in birefringent optical fiber.

Acknowledgments

This work was supported by the National Research Laboratory Project of Korea, and the National R&D Project for Nano Science and Technology.

#3984 - $15.00 US Received 5 March 2004; revised 19 April 2004; accepted 20 April 2004